

Learning Interpretable Characteristic Kernels via Decision Forests

Sambit Panda^{1,†}, Cencheng Shen^{2,†}, and Joshua T. Vogelstein^{1,*}

Abstract. Decision forests are popular tools for classification and regression. These forests naturally generate proximity matrices that measure the frequency of observations appearing in the same leaf node. While other kernels are known to have strong theoretical properties such as being characteristic, there is no similar result available for decision forest-based kernels. In addition, existing approaches to independence and k-sample testing may require unfeasibly large sample sizes and are not interpretable. In this manuscript, we prove that the decision forest induced proximity is a characteristic kernel, enabling consistent independence and k-sample testing via decision forests. We leverage this to introduce kernel mean embedding random forest (KMERF), which is a valid and consistent method for independence and k-sample testing. Our extensive simulations demonstrate that KMERF outperforms other tests across a variety of independence and two-sample testing scenarios. Additionally, the test is interpretable, and its key features are readily discernible. This work therefore demonstrates the existence of a test that is both more powerful and more interpretable than existing methods, flying in the face of conventional wisdom of the trade-off between the two.

1 Introduction Decision forests are ensemble method popularized by Breiman [5]. It is highly effective in classification and regression tasks, particularly in high-dimensional settings [7, 8, 39]. This is achieved by randomly partitioning the feature set and using subsampling techniques to construct multiple decision trees from the training data. To measure the similarity between two observations, a proximity matrix can be constructed, defined as the percentage of trees in which both observations lie in the same leaf node [6]. This proximity matrix serves as an induced kernel or similarity matrix for the decision forest. In general, any random partition algorithm may produce such a kernel matrix.

As the complexity of datasets grow, it becomes increasingly necessary to develop methods that can efficiently perform independence and k-sample testing. We also desire methods that are interpretable, lending insight into how and why statistically significant results were determined. Parametric methods are often highly interpretable, such as Pearson’s correlation and its rank variants [18, 24, 35]. These methods are still popular to detect linear and monotonic relationships in univariate settings, but they are not consistent for detecting more complicated nonlinear relationships. Nonparametric methods can be very powerful. The more recent distance correlation (Dcorr) [37, 38] and the kernel correlation (HSIC) [12, 13] are consistent for testing independence against any distribution of finite second moments for any finite dimensionality; moreover, the energy-based statistics (such as Dcorr) and kernel-based statistics (such as HSIC) are known to be exactly equivalent for all finite samples [23, 32]. The theory supporting universal consistency of these methods (which we refer to as kernel methods hereafter, without loss of generality) depends on those kernels being characteristic kernel [20, 21, 30, 32]. Unfortunately, the above tests do not attempt to further characterize the dependency structure. To the best of our knowledge, very few tests exist [17, 40].

In addition, although these methods all have asymptotic guarantees, for finite samples, performance can be impaired by poorly choosing a particular characteristic kernel. Choosing an appropriate kernel that properly summarize geometries within the data is often times non-obvious [29]. High-dimensional data is particularly vexing [27, 40], and a number of extensions have been proposed to achieve better power such as adaptive metric kernel choice [14], low-dimensional projections [16], and marginal correlations [31].

In this paper, we leverage the popular random forest method [5] and a recent chi-square test [34] for a more powerful and interpretable method for hypothesis testing. We prove that the random for-

¹Johns Hopkins University (JHU), ²University of Delaware.

[†] denotes equal contribution, * corresponding author: jovo@jhu.edu.

est induced kernel is a characteristic kernel, and the resulting kernel mean embedding random forest (KMERF) is a valid and consistent method for independence and k-sample testing. We then demonstrate its empirical advantage over existing tools for high-dimensional testing in a variety of dependence settings, suggesting that it will often be more powerful than existing approaches in real data. As random forest can directly estimate feature importances [5], the outputs of KMERF are also interpretable, KMERF therefore flies in the face of conventional wisdom that one must choose between power and interpretability: KMERF is both empirically more powerful and more interpretable than existing approaches.

2 Preliminaries

2.1 Hypothesis Testing The testing independence hypothesis is formulated as follows: suppose $x_i \in \mathbb{R}^p$ and $y_i \in \mathbb{R}^q$, and n samples of $(x_i, y_i) \stackrel{iid}{\sim} F_{XY}$, i.e., x_i and y_i are realizations of random variables X and Y . The hypothesis for testing independence is

$$\begin{aligned} H_0 &: F_{XY} = F_X F_Y, \\ H_A &: F_{XY} \neq F_X F_Y. \end{aligned}$$

Given any kernel function $k(\cdot, \cdot)$, we can formulate the kernel induced correlation measure as $c_k^n(\mathbf{x}, \mathbf{y})$ using the sample kernel matrices [12, 32], where $\mathbf{x} = \{x_i\}$ and $\mathbf{y} = \{y_i\}$. When the kernel function $k(\cdot, \cdot)$ is characteristic, it has been shown that $c_k^n(\mathbf{x}, \mathbf{y}) \rightarrow 0$ if and only if \mathbf{x} and \mathbf{y} are independent [12].

The k-sample hypothesis is formulated as follows: let $w_i^j \in \mathbb{R}^p$ be the realization of random variable U_j for $j = 1, \dots, l$ and $i = 1, \dots, n_j$. Suppose the l datasets that are sampled i.i.d. from F_1, \dots, F_l and independently from one another. Then,

$$\begin{aligned} H_0 &: F_1 = F_2 = \dots = F_l, \\ H_A &: \exists j \neq j' \text{ s.t. } F_j \neq F_{j'}. \end{aligned}$$

By concatenating the l datasets and introducing an auxiliary random variable, the kernel correlation measure can be used for k-sample testing [23].

2.2 Characteristic Kernel

Definition 1. Let \mathcal{X} be a separable metric space, such as \mathbb{R}^p . A kernel function $k(\cdot, \cdot) : \mathcal{X} \times \mathcal{X} \rightarrow \mathbb{R}$ measures the similarity between two observations in \mathcal{X} , and an $n \times n$ kernel matrix for $\{x_i \in \mathcal{X}, i = 1, \dots, n\}$ is defined by $\mathbf{K}(i, j) = k(x_i, x_j)$.

- A kernel $k(\cdot, \cdot) : \mathcal{X} \times \mathcal{X} \rightarrow \mathbb{R}$ is positive definite if, for any $n \geq 2$, $x_1, \dots, x_n \in \mathcal{X}$ and $a_1, \dots, a_n \in \mathbb{R}$, it satisfies

$$\sum_{i,j=1}^n a_i a_j k(x_i, x_j) \geq 0.$$

- A characteristic kernel is a positive definite kernel that has the following property: for any two random variables X_1 and X_2 with distributions F_{X_1} and F_{X_2} ,

$$(2.1) \quad E[k(\cdot, X_1)] = E[k(\cdot, X_2)] \text{ if and only if } F_{X_1} = F_{X_2}.$$

3 KMERF The proposed approach for hypothesis testing, KMERF, involves the following steps:

1. Run random forest with m trees, with independent bootstrap samples of size $n_b \leq n$ used to construct each tree. The tree structures (partitions) within the forest \mathbf{P} are denoted as $\phi_w \in \mathbf{P}$, where $w \in 1, \dots, m$ and $\phi_w(x_i)$ represents the partition assigned to x_i .

2. Calculate the proximity kernel by

$$\mathbf{K}_{ij}^{\mathbf{x}} = \frac{1}{m} \sum_{w=1}^m [\mathbf{I}(\phi_w(x_i) = \phi_w(x_j))],$$

where $\mathbf{I}(\cdot)$ is the indicator function that checks whether the two observations lie in the same partition in each tree.

3. Compute the unbiased kernel transformation [34, 36] on $\mathbf{K}^{\mathbf{x}}$. Namely, let

$$\mathbf{L}_{ij}^{\mathbf{x}} = \begin{cases} \mathbf{K}_{ij}^{\mathbf{x}} - \frac{1}{n-2} \sum_{t=1}^n \mathbf{K}_{it}^{\mathbf{x}} - \frac{1}{n-2} \sum_{s=1}^n \mathbf{K}_{sj}^{\mathbf{x}} + \frac{1}{(n-1)(n-2)} \sum_{s,t=1}^n \mathbf{K}_{st}^{\mathbf{x}} & i \neq j \\ 0 & i = j \end{cases}$$

4. Let $\mathbf{K}^{\mathbf{y}}$ be the Euclidean distance induced kernel by Shen and Vogelstein [32], or the proximity kernel in the case that dimensions of \mathbf{x} and \mathbf{y} is the same, that is $p = q$, and compute $\mathbf{L}^{\mathbf{y}}$ using the same unbiased transformation. Then the KMERF statistic for the induced kernel k is,

$$c_k^n(\mathbf{x}, \mathbf{y}) = \frac{1}{n(n-3)} \text{tr}(\mathbf{L}^{\mathbf{x}} \mathbf{L}^{\mathbf{y}}).$$

5. Compute the p-value via the following chi-square test [34]:

$$p = 1 - F_{\chi_1^2-1} \left(n \cdot \frac{c_k^n(\mathbf{x}, \mathbf{y})}{\sqrt{c_k^n(\mathbf{x}, \mathbf{x}) \cdot c_k^n(\mathbf{y}, \mathbf{y})}} \right),$$

where χ_1^2 is the chi-square distribution of degree 1. Reject the independence hypothesis if the p-value is less than a specified type 1 error level, say 0.05.

In the numerical implementation, the standard supervised random forest is used with $m = 500$ (which is also applicable to the unsupervised version or other random forest variants [1, 4, 39]). In the second step, we simply compute the proximity kernel defined by the random forest induced kernel. In the third step, we normalize the proximity kernel to ensure it obtains a consistent dependence measure; this is the KMERF test statistic. We found that utilizing the multiscale version of the kernel correlation [33, 40], which is equivalent for linear relationships while being better for nonlinear relationships, produced similar results to using distance correlation, but substantially increased runtimes.

Note that one could also compute a p-value for KMERF via the permutation test, which is a standard procedure for testing independence [11]. Specifically, first compute a kernel on the observed $\{x_i\}$ and $\{y_i\}$. Then randomly permute the index of $\{y_i\}$, repeat the kernel generation process for $\{y_i\}$ for each permutation. This process involves training a new random forest for each permutation. Finally, compute the test statistic for each of the permutations, and the p-value equals the percentage the permuted statistics that are larger than the observed statistic. However, the permutation test is very slow for large sample size and almost always yields similar results as the chi-square test.

4 Theoretical Properties Here, we show that the random forest kernel characteristic, and the induced test statistic used in KMERF allows for valid and universally consistent independence and k-sample testing. All proofs are in appendix.

For a kernel to be characteristic, it first needs to be positive definite, which is indeed the case for the forest-induced kernel:

Theorem 2. *The random forest induced kernel $\mathbf{K}^{\mathbf{x}}$ is always positive definite.*

This theorem holds because the forest-induced kernel is a summation of a permuted block diagonal matrix, with each matrix coming from individual tree, that is positive definite [9]; and a summation of positive definite matrices is still positive definite.

Next, we show the kernel is characteristic when the tree partition area converges to zero. A similar property is also used for proving classification consistency for k-nearest-neighbors [10], and we shall denote $N(\phi_w)$ as the maximum area of each part.

Theorem 3. *Suppose as $n, m \rightarrow \infty$, $N(\phi_w) \rightarrow 0$ for each tree $\phi_w \in \mathbf{P}$ and each observation x_i . Then the random forest induced kernel \mathbf{K}^x is asymptotically characteristic.*

Intuitively, for sufficiently many trees and sufficiently small leaf region, observations generated by two different distributions cannot always be in the same leaf region.

This leads to the validity and consistency result of KMERF:

Corollary 4. *KMERF satisfies*

$$\lim_{n \rightarrow \infty} c_k^n(\mathbf{x}, \mathbf{y}) = c \geq 0,$$

with equality to 0 if and only if $F_{XY} = F_X F_Y$. Moreover, for sufficiently large n and sufficiently small type 1 error level α , this method is valid and consistent for independence and k-sample testing.

By Gretton et al. [12], any characteristic-kernel based dependence measure converges to 0 if and only if X and Y are independent. Moreover, Shen et al. [34] showed that the chi-square distribution $\chi_1^2 - 1$ approximates and upper-tail dominates the true null distribution of any unbiased kernel when using distance correlation, making it a valid and consistent test.

5 Simulations In this section we exhibit the consistency and validity of KMERF, and compare its testing power with other competitors in a comprehensive simulation set-up. We utilize the `hyppo` package in Python [22], which uses `scikit-learn` [25] random forest with 500 trees and otherwise default hyper-parameters, and calculate the proximity matrix from this. The KMERF statistic and p-value then computed via the process in Section 3. The mathematical details for each simulation type is in the Appendix C.

5.1 Testing Independence In this section we compare KMERF to Multiscale Graph Correlation (MGC), Distance Correlation (Dcorr), Hilbert-Schmidt Independence Criterion (Hsic), and Heller-Heller-Gorfine (HHG) method, Canonical Correlation Analysis (CCA), and the RV coefficient. The HHG method has been shown to work extremely well against nonlinear dependencies [15]. The MGC method has been shown to work well against linear, nonlinear, and high-dimensional dependencies [33]. The CCA and RV coefficients are popular multivariate extensions of Pearson correlation. For each method, we use the corresponding implementation in `hyppo` with default settings.

We take 20 high-dimensional simulation settings [40], consisting of various linear, monotone, and strongly nonlinear dependencies with p increasing, $q = 1$, and $n = 100$. To estimate the testing power in each setting, we generate dependent (x_i, y_i) for $i = 1, \dots, n$, compute the test statistic for each method, repeat for $r = 10000$ times. Via the empirical alternative and null distribution of the test statistic, we estimate the testing power of each method at type 1 error level of $\alpha = 0.05$. The power result is shown in Figure 1 shows that KMERF achieves superior performance for most simulation modalities, except a few like circle and ellipse.

5.2 Two Sample Testing Here, we compare the performance in the two-sample testing regime. It has been shown that all independence measures can be used for two-sample testing [23, 32], allowing all previous independence testing methods to be compared here as well. Once again, we investigate statistical power differences with 20 simulation settings consisting of various linear and nonlinear, monotonic and nonmonotonic functions with dimension increasing from $p = 3, \dots, 10$, $q = 1$, and $n = 100$. We then apply a random rotation to this generated simulation and generate the second independent sample (via a rigid transformation).

Figure 2 shows that, once again, for the majority of simulations settings, KMERF performs at or better than other tests in nearly all simulations and simulation dimensions. For certain simulation set-

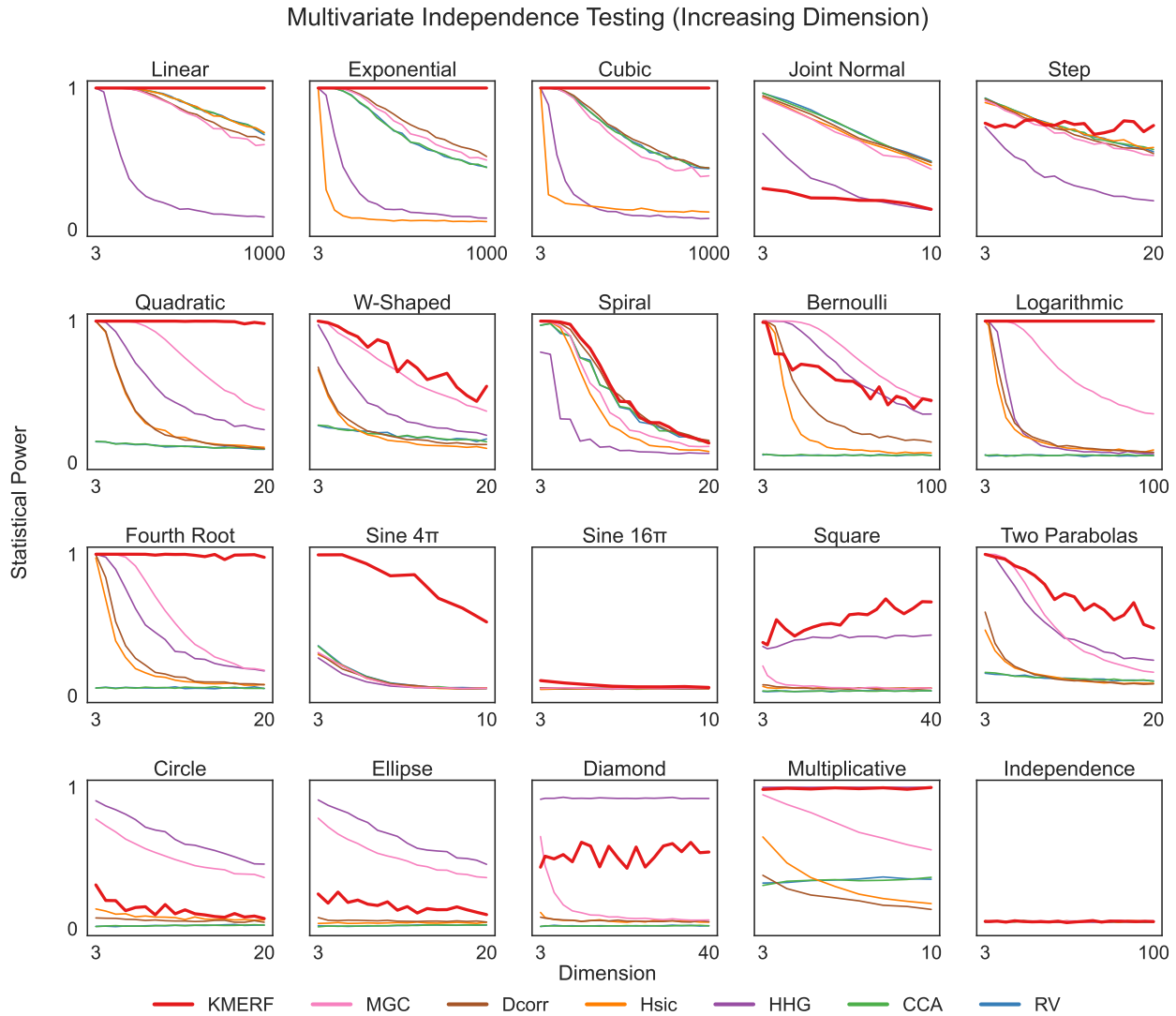


Figure 1: Multivariate independence testing power for 20 different settings with increasing p , fixed $q = 1$, and $n = 100$. For the majority of the simulations and simulation dimensions, KMERF performs as well as, or better than, existing multivariate independence tests in high-dimensional dependence testing.

tings, especially the exponential, cubic, and fourth root, KMERF vastly outperforms other metrics as dimensions increases.

5.3 Interpretability Not only does KMERF typically offer empirically better statistical power compared to alternatives, it also offers insights into which features are the most important within the data set. Figure 3 shows normalized 95% confidence intervals of relative feature importances for each simulation, where the black line shows the mean and the light grey line shows the 95% confidence interval. Mean and individual tree feature importances were normalized using min-max feature scaling. The simulations were modified such that the weighting of each feature decreased as feature importance increased, with the expectation that the algorithm would detect a decrease in feature importance as dimension increased. With these simulations, we are able to determine that exact feature importance trend, except for a few of the more complex simulations. The process we used to generate this figure can be trivially extended to a two-sample or k-sample case.

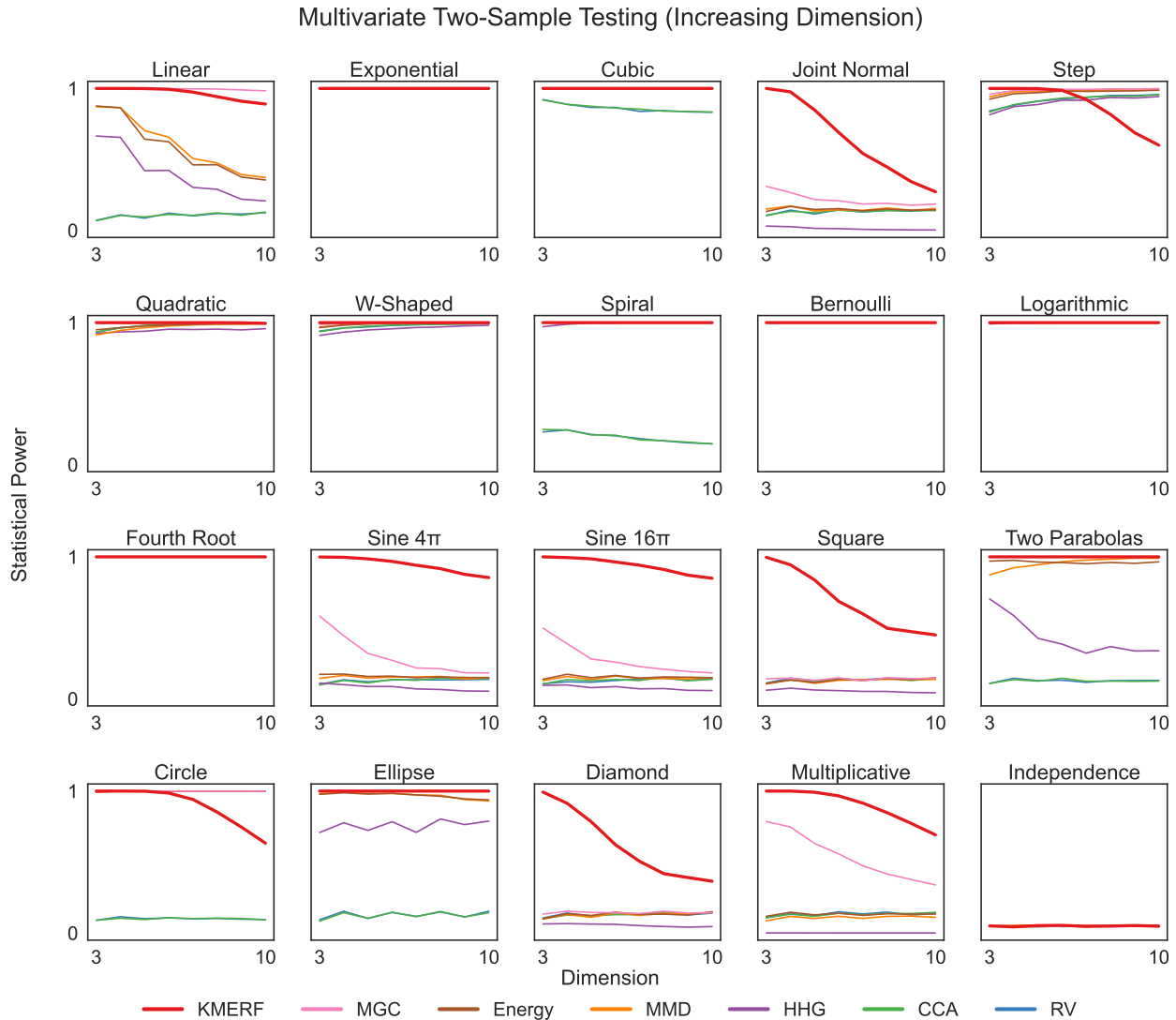


Figure 2: Multivariate two-sample testing power for 20 different settings with increasing p , fixed $q = 1$, and $n = 100$. For nearly all simulations and simulation dimensions, KMERF performs as well as, or better than, existing multivariate two-sample tests in high-dimensional dependence testing.

6 Real Data We then applied KMERF to a data set consisting of proteolytic peptides derived from the blood samples of 95 individuals harboring pancreatic ($n=10$), ovarian ($n=24$), colorectal cancer ($n=28$), and healthy controls ($n=33$) [40]. The processed data included 318 peptides derived from 121 proteins (see Appendix D for full details). Figure 4 shows the p-values for KMERF between pancreatic and healthy subjects compared to the p-values for KMERF between pancreatic cancer and all other subjects. The test identifies neurogranin as a potentially valuable marker for pancreatic cancer, which the literature also corroborates [44, 45]. Meanwhile, while some of the other tests identified this biomarker, they identified others that are upregulated in other types of cancers as well (false positives). We also show in the figure that the biomarker chosen by KMERF provides better true positive detection when compared to the other tests (there is no ground truth in this case, so a leave-one-out k-nearest-neighbor classification approach was used instead).

7 Discussion KMERF is, to the best of our knowledge, one of the first learned kernel that is proven to be characteristic. The empirical experiments presented here illustrate the potential advantages of learning kernels, specifically for independence and k-sample testing.

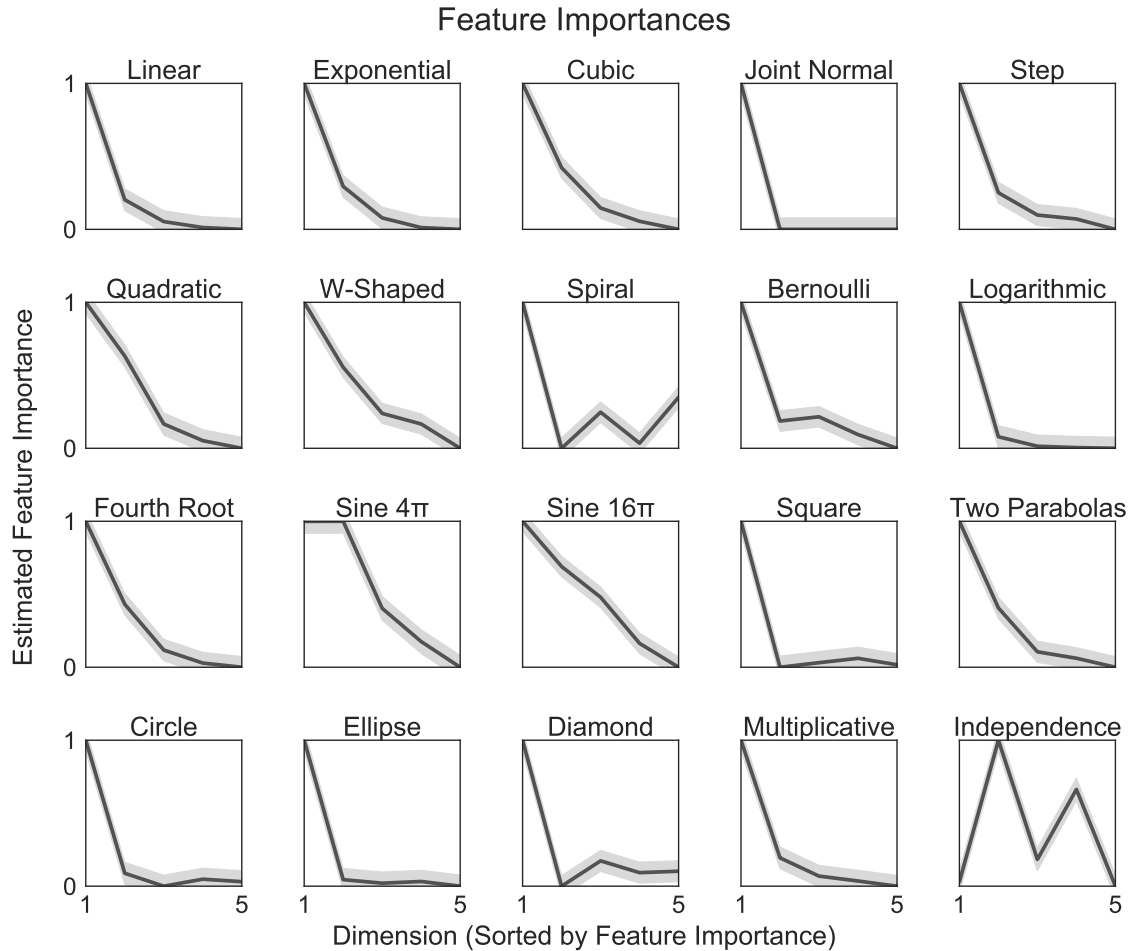


Figure 3: Normalized mean (black) and 95% confidence intervals (light grey) using min-max normalization for relative feature importances derived from random forest over five dimensions for each simulation tested for 100 samples. The features were sorted from most to least informative for all simulations except for the Independence simulation). As expected, estimated feature importance decreases as dimension increases. A feature of KMERF is insights into interpretability, and we show here which dimensions of our simulations influence the outcome of independence test the most.

In fact, multiscale graph correlation [33, 40] can be thought of, in a sense, as kernel learning: given n samples, and a pair of kernel or distance functions, it chooses one of the approximately n^2 sparsified kernels, by excluding all but the nearest neighbors for each data point [33, 40]. Because random forest can be thought of as a nearest neighbor algorithm [19], in a sense, the forest induced kernel is a natural extension of Vogelstein et al. [40], which leads to far more data-adaptive estimates of the nearest neighbors using supervised information. Moreover, proving that the random-forest induced kernel is characteristic is a first step towards building lifelong learning kernel machines with strong theoretical guarantees [26, 41].

As the choice of kernel is crucial for empirical performance, this manuscript offers a new kernel construction that is not only universally consistent for testing independence, but also exhibits strong empirical advantages, especially for high-dimensional testing. What is unique to this choice of kernel is the robustness and interpretability. It will be worthwhile to further understand the underlying theoretical mechanism of the induced characteristic kernel, as well as evaluating the performance of these forest induced kernels on other learning problems, including classification, regression, clustering, and embedding [28].

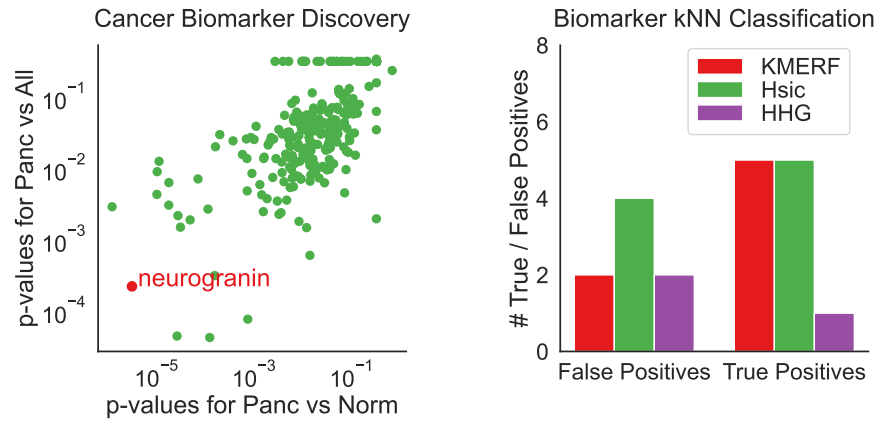


Figure 4: (A) For each peptide, the p-values for testing dependence between pancreatic and healthy subjects by KMERF is compared to the p-value for testing dependence between pancreatic and all other subjects. At the critical level 0.05, KMERF identifies a unique protein. (B) The true and false positive counts using a k-nearest neighbor (choosing the best $k \in [1, 10]$) leave-one-out classification using only the significant peptides identified by each method. The peptide identified by KMERF achieves the best true and false positive rates.

Acknowledgment This work was partially supported by the Child Mind Institute Endeavor Scientist Program, the National Science Foundation Division of Mathematical Sciences award DMS-1712947, DMS-2113099, the National Security Science and Engineering Faculty Fellowship (NSSEFF), the Johns Hopkins University Human Language Technology Center of Excellence (JHU HLT COE), and the Defense Advanced Research Projects Agency's (DARPA) SIMPLEX program through SPAWAR contract N66001-15-C-4041, the XDATA program of DARPA administered through Air Force Research Laboratory contract FA8750-12-2-0303, the Office of Naval Research contract N00014-12-1-0601, the Air Force Office of Scientific Research contract FA9550-14-1-0033. The authors thank Dr. Minh Tang, Dr. Shangsi Wang, Dr. Eliza O'Reilly, and anonymous reviewers for their suggestions and comments in improving the paper.

References

- [1] S. Athey, J. Tibshirani, and S. Wager. Generalized random forests. *Annals of Statistics*, 47(2): 1148–1178, 2018.
- [2] Y. Benjamini and Y. Hochberg. Controlling the false discovery rate: a practical and powerful approach to multiple testing. *Journal of the royal statistical society. Series B (Methodological)*, pages 289–300, 1995.
- [3] P. J. Bickel and K. A. Doksum. *Mathematical Statistics: Basic Ideas and Selected Topics, Vol I*. Prentice Hall, 2nd edition, 2006.
- [4] R. Blaser and P. Fryzlewicz. Random rotation ensembles. *Journal of Machine Learning Research*, 17(4):1–26, 2016.
- [5] L. Breiman. Random forests. *Machine Learning*, 4(1):5–32, October 2001.
- [6] L. Breiman. Some infinity theory for predictor ensembles. *Journal of Combinatorial Theory, Series A*, 98:175–191, 2002.
- [7] R. Caruana and A. Niculescu-Mizil. An empirical comparison of supervised learning algorithms. In *Proceedings of the 23rd international conference on Machine learning*, pages 161–168. ACM, 2006.
- [8] R. Caruana, N. Karampatziakis, and A. Yessenalina. An empirical evaluation of supervised learning in high dimensions. *Proceedings of the 25th International Conference on Machine Learning*, 2008.
- [9] A. Davies and Z. Ghahramani. The random forest kernel and creating other kernels for big data from random partitions. *arXiv:1402.4293v1*, 2014.
- [10] L. Devroye, L. Györfi, and G. Lugosi. *A Probabilistic Theory of Pattern Recognition*. Springer, 1996.
- [11] P. Good. *Permutation, Parametric, and Bootstrap Tests of Hypotheses*. Springer, 2005.
- [12] A. Gretton, R. Herbrich, A. Smola, O. Bousquet, and B. Schölkopf. Kernel methods for measuring independence. *Journal of Machine Learning Research*, 6:2075–2129, 2005.
- [13] A. Gretton, K. M. Borgwardt, M. J. Rasch, B. Schölkopf, and A. Smola. A Kernel Two-Sample Test. *Journal of Machine Learning Research*, 13(25):723–773, 2012. ISSN 1533-7928.
- [14] A. Gretton, D. Sejdinovic, H. Strathmann, S. Balakrishnan, M. M. Pontil, K. Fukumizu, and B. K. Sriperumbudur. Optimal kernel choice for large-scale two-sample tests. In *Advances in neural information processing systems 25*, pages 1205–1213, 2012.
- [15] R. Heller, Y. Heller, and M. Gorfine. A consistent multivariate test of association based on ranks of distances. *Biometrika*, 100(2):503–510, 2013.
- [16] C. Huang and X. Huo. A statistically and numerically efficient independence test based on random projections and distance covariance. *arXiv*, 2017.
- [17] W. Jitkrittum, Z. Szabó, K. P. Chwiałkowski, and A. Gretton. Interpretable distribution features with maximum testing power. In *Advances in Neural Information Processing Systems*, pages 181–189, 2016.
- [18] M. G. Kendall. *Rank Correlation Methods*. London: Griffin, 1970.
- [19] Y. Lin and Y. Jeon. Random forests and adaptive nearest neighbors. *J. Am. Stat. Assoc.*, 101(474):578–590, 2006.
- [20] R. Lyons. Distance covariance in metric spaces. *Annals of Probability*, 41(5):3284–3305, 2013.
- [21] R. Lyons. Errata to “distance covariance in metric spaces”. *Annals of Probability*, 46(4):2400–2405, 2018.
- [22] S. Panda, S. Palaniappan, J. Xiong, E. W. Bridgeford, R. Mehta, C. Shen, and J. T. Vogelstein. *hyppo: A comprehensive multivariate hypothesis testing python package*, 2020.
- [23] S. Panda, C. Shen, R. Perry, J. Zorn, A. Lutz, C. E. Priebe, and J. T. Vogelstein. *Nonpar manova via independence testing*, 2021.
- [24] K. Pearson. Notes on regression and inheritance in the case of two parents. *Proceedings of the*

- Royal Society of London, 58:240–242, 1895.
- [25] F. Pedregosa, G. Varoquaux, A. Gramfort, V. Michel, B. Thirion, O. Grisel, M. Blondel, P. Prettenhofer, R. Weiss, V. Dubourg, J. Vanderplas, A. Passos, D. Cournapeau, M. Brucher, M. Perrot, and Édouard Duchesnay. Scikit-learn: Machine learning in python. Journal of Machine Learning Research, 12(85):2825–2830, 2011. URL <http://jmlr.org/papers/v12/pedregosa11a.html>.
- [26] A. Pentina and S. Ben-David. Multi-task and lifelong learning of kernels. In Algorithmic Learning Theory, pages 194–208. Springer International Publishing, 2015.
- [27] A. Ramdas, S. J. Reddi, B. Póczos, A. Singh, and L. Wasserman. On the decreasing power of kernel and distance based nonparametric hypothesis tests in high dimensions. In 29th AAAI Conference on Artificial Intelligence, 2015.
- [28] B. Schölkopf and A. J. Smola. Learning with kernels: support vector machines, regularization, optimization, and beyond. MIT press, 2002.
- [29] D. Sejdinovic, A. Gretton, B. Sriperumbudur, and K. Fukumizu. Hypothesis testing using pairwise distances and associated kernels (with appendix). arXiv preprint arXiv:1205.0411, 2012.
- [30] D. Sejdinovic, B. Sriperumbudur, A. Gretton, and K. Fukumizu. Equivalence of distance-based and rkhs-based statistics in hypothesis testing. Annals of Statistics, 41(5):2263–2291, 2013.
- [31] C. Shen. Scaling up independence testing: Maximum marginal distance correlation and the chi-square test. <https://arxiv.org/abs/2001.01095>, 2023.
- [32] C. Shen and J. T. Vogelstein. The exact equivalence of distance and kernel methods in hypothesis testing. AStA Advances in Statistical Analysis, 105(3):385–403, 2021.
- [33] C. Shen, C. E. Priebe, and J. T. Vogelstein. From distance correlation to multiscale graph correlation. Journal of the American Statistical Association, 115(529):280–291, 2020.
- [34] C. Shen, S. Panda, and J. T. Vogelstein. The chi-square test of distance correlation. Journal of Computational and Graphical Statistics, 31(1):254–262, 2022.
- [35] C. Spearman. The Proof and Measurement of Association between Two Things. The American Journal of Psychology, 15(1):72, 1904. ISSN 00029556. doi: 10.2307/1412159. URL <http://www.jstor.org/stable/1412159?origin=crossref>.
- [36] G. Székely and M. Rizzo. Partial distance correlation with methods for dissimilarities. Annals of Statistics, 42(6):2382–2412, 2014.
- [37] G. Székely and M. L. Rizzo. The distance correlation t-test of independence in high dimension. Journal of Multivariate Analysis, 117:193–213, 2013.
- [38] G. Székely, M. L. Rizzo, and N. K. Bakirov. Measuring and testing independence by correlation of distances. Annals of Statistics, 35(6):2769–2794, 2007.
- [39] T. Tomita, J. Browne, C. Shen, J. Chung, J. Patsolic, B. Falk, J. Yim, C. E. Priebe, R. Burns, M. Maggioni, and J. T. Vogelstein. Sparse projection oblique randomer forests. Journal of Machine Learning Research, 21(104):1–39, 2020.
- [40] J. T. Vogelstein, Q. Wang, E. W. Bridgeford, C. E. Priebe, M. Maggioni, and C. Shen. Discovering and deciphering relationships across disparate data modalities. eLife, 8:e41690, 2019.
- [41] J. T. Vogelstein, J. Dey, H. S. Helm, W. LeVine, R. D. Mehta, T. M. Tomita, H. Xu, A. Geisa, Q. Wang, G. M. van de Ven, C. Gao, W. Yang, B. Tower, J. Larson, C. M. White, and C. E. Priebe. Representation ensembling for synergistic lifelong learning with quasilinear complexity, 2023.
- [42] Q. Wang, R. Chaerkady, J. Wu, H. J. Hwang, N. Papadopoulos, L. Kopelovich, A. Maitra, H. Matthaei, J. R. Eshleman, R. H. Hruban, et al. Mutant proteins as cancer-specific biomarkers. Proceedings of the National Academy of Sciences, 108(6):2444–2449, 2011.
- [43] Q. Wang, M. Zhang, T. Tomita, J. T. Vogelstein, S. Zhou, N. Papadopoulos, K. W. Kinzler, and B. Vogelstein. Selected reaction monitoring approach for validating peptide biomarkers. Proceedings of the National Academy of Sciences, 114(51):13519–13524, 2017.
- [44] E. A. Willemse, A. De Vos, E. M. Herries, U. Andreasson, S. Engelborghs, W. M. Van Der Flier, P. Scheltens, D. Crimmins, J. H. Ladenson, E. Vanmechelen, et al. Neurogranin as cerebrospinal

fluid biomarker for alzheimer disease: an assay comparison study. Clinical chemistry, 64(6):927–937, 2018.

- [45] J. Yang, F. K. Korley, M. Dai, and A. D. Everett. Serum neurogranin measurement as a biomarker of acute traumatic brain injury. Clinical biochemistry, 48(13-14):843–848, 2015.

Appendix A. Proofs.

Theorem 1. *The random forest induced kernel \mathbf{K}^x is always positive definite.*

Proof. The forest-induced kernel is a summation of permuted block diagonal matrix, with ones in each block and zeros elsewhere [9], i.e.,

$$\mathbf{K}^x = \frac{1}{m} \sum_{w=1}^m Q_w B_w Q_w^T,$$

where Q is a permutation matrix, and B is a block diagonal matrix with each block representing a leaf node, and the sum is over all m trees in the forest. For example, when each leaf node only contains one observation, B becomes the identity matrix.

Each block matrix is always positive definite and still positive definite after permutation, because permutation does not change eigenvalues. As summation of positive definite matrices is still positive definite, \mathbf{K}^x is always positive definite. ■

Next we show the kernel can be characteristic, when the tree partition area converges to zero. A similar property is also used for proving classification consistency in k -nearest-neighbor [10], and we shall denote $N(\phi_w) \in \mathbb{R}_{\geq 0}^{L_w}$ as the maximum area of each part.

Theorem 2. *Suppose as $n, m \rightarrow \infty$, $N(\phi_w) \rightarrow 0$ for each tree $\phi_w \in \mathbf{P}$ and each observation x_i . Then the random forest induced kernel \mathbf{K}^x is asymptotically characteristic.*

Proof. since the kernel is positive semidefinite, it suffices to prove

$$(A.1) \quad E[k(\cdot, X_1)] = E[k(\cdot, X_2)] \text{ if and only if } F_{X_1} = F_{X_2}.$$

The forward implication is trivial. To prove the converse, it suffices to investigate when $E[\mathbf{K}^x(\cdot, X_1)] = E[\mathbf{K}^x(\cdot, X_2)]$, or equivalently

$$E_{X_1} \left(\frac{1}{m} \sum_{w=1}^m [\mathbf{I}(\phi_w(X_1) = \phi_w(z))] \right) = E_{X_2} \left(\frac{1}{m} \sum_{w=1}^m [\mathbf{I}(\phi_w(X_2) = \phi_w(z))] \right)$$

for any observation z .

We first show the above equality occurs if and only if $\phi_w(X_1) \stackrel{D}{=} \phi_w(X_2)$. Once again, the forward implication is trivial. The converse can be shown by contradiction: without loss of generality, suppose there exists a leaf node region U such that $\phi_w(X_1) \in U$ with probability p_1 while $\phi_w(X_2) \in U$ with probability p_2 . Then for any point-mass observation z always in U , $E[\mathbf{K}^x(z, X_1)] = p_1 \neq E[\mathbf{K}^x(z, X_2)] = p_2$, which is a contradiction.

Next we show $\phi_w(X_1) \stackrel{D}{=} \phi_w(X_2)$ if and only if $F_{X_1} = F_{X_2}$. The forward implication is again trivial. The converse is shown by contradiction. Suppose $F_{X_1} \neq F_{X_2}$. Without loss of generality, there always exists a neighborhood $N(x)$ such that $Prob(X_1 \in N(x)) = p_3 \neq Prob(X_2 \in N(x)) = p_4$. Now, because each tree partition area converges to 0, we can always make $N(x)$ small enough so that $\phi_w(N(x)) = U$ almost surely for some leaf node region U . Then $Prob(\phi_w(X_1) = U) = p_3 \neq Prob(\phi_w(X_2) = U) = p_4$. Thus $\phi_w(X_1) \not\stackrel{D}{=} \phi_w(X_2)$, contradiction. Therefore, Equation 1 is proved, and the kernel is characteristic. ■

Corollary 3. *KMERF satisfies*

$$\lim_{n \rightarrow \infty} c_k^n(\mathbf{x}, \mathbf{y}) = c \geq 0,$$

with equality to 0 if and only if $F_{XY} = F_X F_Y$. Moreover, for sufficiently large n and sufficiently small type 1 error level α , this method is valid and consistent for independence and k -sample testing.

Proof. As $n \rightarrow \infty$, \mathbf{K} is asymptotically a characteristic kernel by Theorem 3. By Shen and Vogelstein [32], the Euclidean distance induced kernel is also characteristic. Therefore by Gretton et al. [12], Lyons [20], $c_k^n(\mathbf{x}, \mathbf{y})$ is asymptotically 0 if and only if independence.

By Shen et al. [34], for sufficiently large n , the chi-square distribution $\frac{\chi_1^2 - 1}{n}$ dominates the true null distribution of the unbiased correlation in upper tail. Therefore, when X and Y are actually independent, the testing power is no more than the type 1 error level α , making it a valid test. When X and Y are dependent, the distribution $\frac{\chi_1^2 - 1}{n}$ converges to 0 in probability, such that the p-value converges to 0 and the testing power converges to 1, making it a consistent test. ■

Appendix B. Limitations. There are a few limitations to this approach. In the problem setting that we are considering (composite null vs. composite alternative), there is no uniformly most powerful test [3]. So, while this paper presents its argument with simulated data, it is not yet known how this statistical method will perform against other statistics with real data. This is difficult to determine as distributions of data are oftentimes unknown and so may not fall cleanly in one of the 20 distributions that were tested. Given the performance of KMERF, it is likely safer to use KMERF over others as it appears to perform better than alternatives in most cases.

In addition, we have currently have not explored the performance of our algorithm with respect to other decision forests types [1, 4, 39], and hyper-parameter tuning. It would be interesting the extend this approach using these decision forests to answer additional hypothesis testing problems, such as paired k-sample testing, etc.

Appendix C. Simulations.

C.1 Independence Simulations For the independence simulation, we test independence between X and Y . For the random variable $X \in \mathbb{R}^p$, we denote $X_{|d|}$, $d = 1, \dots, p$ as the d^{th} dimension of X . $w \in \mathbb{R}^p$ is a decaying vector with $w_{|d|} = 1/d$ for each d , such that $w^\top X$ is a weighted summation of all dimensions of X . Furthermore, $\mathcal{U}(a, b)$ denotes the uniform distribution on the interval (a, b) , $\mathcal{B}(p)$ denotes the Bernoulli distribution with probability p , $\mathcal{N}(\mu, \Sigma)$ denotes the normal distribution with mean μ and covariance Σ , U and V represent some auxiliary random variables, κ is a scalar constant to control the noise level, and ϵ is sampled from an independent standard normal distribution unless mentioned otherwise.

1. **Linear**(X, Y) $\in \mathbb{R}^p \times \mathbb{R}$:

$$\begin{aligned} X &\sim \mathcal{U}(-1, 1)^p, \\ Y &= w^\top X + \kappa\epsilon. \end{aligned}$$

2. **Exponential**(X, Y) $\in \mathbb{R}^p \times \mathbb{R}$:

$$\begin{aligned} X &\sim \mathcal{U}(0, 3)^p, \\ Y &= \exp(w^\top X) + 10\kappa\epsilon. \end{aligned}$$

3. **Cubic**(X, Y) $\in \mathbb{R}^p \times \mathbb{R}$:

$$\begin{aligned} X &\sim \mathcal{U}(-1, 1)^p, \\ Y &= 128 \left(w^\top X - \frac{1}{3} \right)^3 + 48 \left(w^\top X - \frac{1}{3} \right)^2 - 12 \left(w^\top X - \frac{1}{3} \right) + 80\kappa\epsilon. \end{aligned}$$

4. **Joint Normal**(X, Y) $\in \mathbb{R}^p \times \mathbb{R}^p$: Let $\rho = 1/2p$, I_p be the identity matrix of size $p \times p$, J_p be the matrix of ones of size $p \times p$, and $\Sigma = \begin{bmatrix} I_p & \rho J_p \\ \rho J_p & (1 + 0.5\kappa) I_p \end{bmatrix}$. Then,

$$(X, Y) \sim \mathcal{N}(0, \Sigma).$$

5. **Step Function** $(X, Y) \in \mathbb{R}^p \times \mathbb{R}$:

$$X \sim \mathcal{U}(-1, 1)^p,$$

$$Y = \mathbb{I}(w^\top X > 0) + \epsilon,$$

where \mathbb{I} is the indicator function; that is, $\mathbb{I}(z)$ is unity whenever z is true, and 0 otherwise.

6. **Quadratic** $(X, Y) \in \mathbb{R}^p \times \mathbb{R}$:

$$X \sim \mathcal{U}(-1, 1)^p,$$

$$Y = (w^\top X)^2 + 0.5\kappa\epsilon.$$

7. **W-Shape** $(X, Y) \in \mathbb{R}^p \times \mathbb{R}$: For $U \sim \mathcal{U}(-1, 1)^p$,

$$X \sim \mathcal{U}(-1, 1)^p,$$

$$Y = 4 \left[\left((w^\top X)^2 - \frac{1}{2} \right)^2 + \frac{w^\top U}{500} \right] + 0.5\kappa\epsilon.$$

8. **Spiral** $(X, Y) \in \mathbb{R}^p \times \mathbb{R}$: For $U \sim \mathcal{U}(0, 5)$, $\epsilon \sim \mathcal{N}(0, 1)$,

$$X_{|d|} = U \sin(\pi U) \cos^d(\pi U) \text{ for } d = 1, \dots, p-1,$$

$$X_{|p|} = U \cos^p(\pi U),$$

$$Y = U \sin(\pi U) + 0.4p\epsilon.$$

9. **Uncorrelated Bernoulli** $(X, Y) \in \mathbb{R}^p \times \mathbb{R}$: For $U \sim \mathcal{B}(0.5)$, $\epsilon_1 \sim \mathcal{N}(0, I_p)$, $\epsilon_2 \sim \mathcal{N}(0, 1)$,

$$X \sim \mathcal{B}(0.5)^p + 0.5\epsilon_1,$$

$$Y = (2U - 1)w^\top X + 0.5\epsilon_2.$$

10. **Logarithmic** $(X, Y) \in \mathbb{R}^p \times \mathbb{R}^p$: For $\epsilon \sim \mathcal{N}(0, I_p)$,

$$X \sim \mathcal{N}(0, I_p),$$

$$Y_{|d|} = 2 \log_2(|X_{|d|}|) + 3\kappa\epsilon_{|d|} \text{ for } d = 1, \dots, p.$$

11. **Fourth Root** $(X, Y) \in \mathbb{R}^p \times \mathbb{R}$:

$$X \sim \mathcal{U}(-1, 1)^p,$$

$$Y = |w^\top X|^{1/4} + \frac{\kappa}{4}\epsilon.$$

12. **Sine Period 4π** $(X, Y) \in \mathbb{R}^p \times \mathbb{R}^p$: For $U \sim \mathcal{U}(-1, 1)$, $V \sim \mathcal{N}(0, 1)^p$, $\theta = 4\pi$,

$$X_{|d|} = U + 0.02pV_{|d|} \text{ for } d = 1, \dots, p,$$

$$Y = \sin(\theta X) + \kappa\epsilon.$$

13. **Sine Period 16π** $(X, Y) \in \mathbb{R}^p \times \mathbb{R}^p$: Same as above except $\theta = 16\pi$ and the noise on Y is changed to $0.5\kappa\epsilon$.

14. **Square** $(X, Y) \in \mathbb{R}^p \times \mathbb{R}^p$: For $U \sim \mathcal{U}(-1, 1)$, $V \sim \mathcal{U}(-1, 1)$, $\epsilon \sim \mathcal{N}(0, 1)^p$, $\theta = -\frac{\pi}{8}$,

$$X_{|d|} = U \cos(\theta) + V \sin(\theta) + 0.05p\epsilon_{|d|},$$

$$Y_{|d|} = -U \sin(\theta) + V \cos(\theta).$$

15. **Diamond** $(X, Y) \in \mathbb{R}^p \times \mathbb{R}^p$: Same as above except $\theta = \pi/4$.

16. **Two Parabolas** $(X, Y) \in \mathbb{R}^p \times \mathbb{R}$: For $\epsilon \sim \mathcal{U}(0, 1)$, $U \sim \mathcal{B}(0.5)$,

$$X \sim \mathcal{U}(-1, 1)^p,$$

$$Y = \left((w^\top X)^2 + 2\kappa\epsilon \right) \cdot \left(U - \frac{1}{2} \right).$$

17. **Circle** $(X, Y) \in \mathbb{R}^p \times \mathbb{R}$: For $U \sim \mathcal{U}(-1, 1)^p$, $\epsilon \sim \mathcal{N}(0, I_p)$, $r = 1$,

$$X_{|d|} = r \left(\sin(\pi U_{|d+1|}) \prod_{j=1}^d \cos(\pi U_{|j|}) \right) \text{ for } d = 1, \dots, p-1,$$

$$X_{|p|} = r \left(\prod_{j=1}^p \cos(\pi U_{|j|}) \right),$$

$$Y = \sin(\pi U_{|1|}) + 0.4\epsilon_{|p|}.$$

18. **Ellipse** $(X, Y) \in \mathbb{R}^p \times \mathbb{R}^p$: Same as above except $r = 5$.

19. **Multiplicative Noise** $(x, y) \in \mathbb{R}^p \times \mathbb{R}^p$: $u \sim \mathcal{N}(0, I_p)$,

$$x \sim \mathcal{N}(0, I_p),$$

$$y_{|d|} = u_{|d|}x_{|d|} \text{ for } d = 1, \dots, p.$$

20. **Multimodal Independence** $(X, Y) \in \mathbb{R}^p \times \mathbb{R}$: For $U \sim \mathcal{N}(0, I_p)$, $V \sim \mathcal{N}(0, I_p)$, $U' \sim \mathcal{B}(0.5)^p$, $V' \sim \mathcal{B}(0.5)^p$,

$$X = U/3 + 2U' - 1,$$

$$Y = V/3 + 2V' - 1.$$

Figure F1 visualizes these equations. The light grey points in the figure are each simulation with noise added and the dark grey points are each simulation without noise added. Note that the last two simulations don't have any noise parameters.

C.2 Two-Sample Simulations We do two-sample testing between Z and Z' , generated as follows: let $Z = [X|Y]$ be the respective random variables from the independence simulation setup. Then define Q_θ as a rotation matrix for a given angle θ , i.e.,

$$Q_\theta = \begin{bmatrix} \cos \theta & 0 & \dots & -\sin \theta \\ 0 & 1 & \dots & 0 \\ \vdots & \vdots & \ddots & \vdots \\ \sin \theta & 0 & \dots & \cos \theta \end{bmatrix}$$

Then we let

$$Z' = Q_\theta Z^\top$$

be the rotated versions of Z .

Independence Simulations

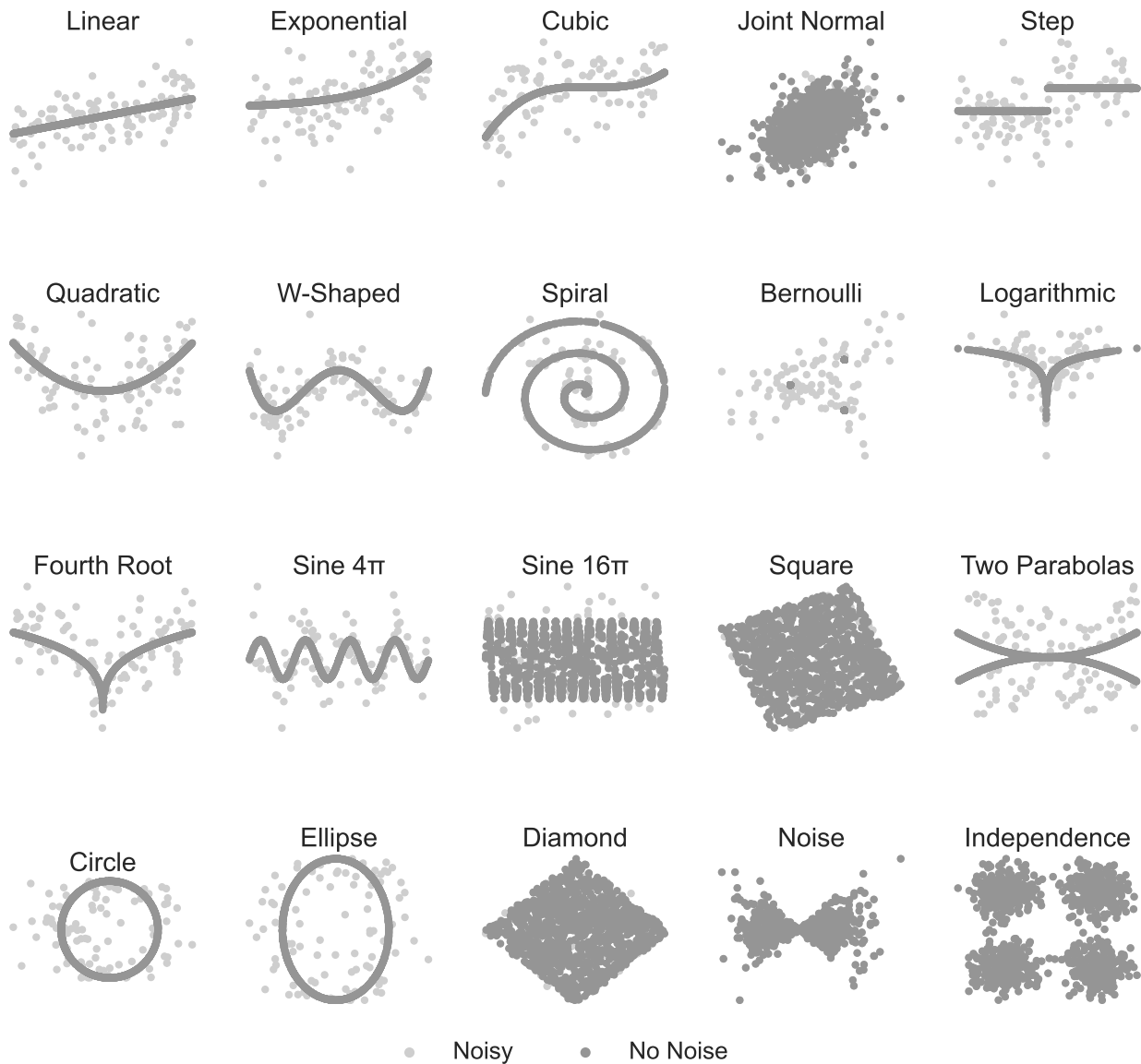


Figure F1: Simulations used for Figures 1 and 3. 100 points from noisy simulations (light grey points) on 1000 points from simulations without noise (dark grey points) for each of the 20 dimensional simulations shown above.

Figure F2 visualizes the above simulations. The simulations light grey points is a simulated data set and the dark grey points are the same dataset rotated by 10 degrees counter-clockwise. Simulations were plotted with min-max normalization for visualization purposes.

Appendix D. Real Data. Previous studies have shown the utility of selection reaction monitoring when measuring protein and peptide abundance [42], and one was used to identify 318 peptides from 33 normal, 10 pancreatic cancer, 28 colorectal cancer, and 24 ovarian cancer samples [43]. For all tests, we created a binary label vector, where 1 indicated presence of pancreatic cancer in the patients and 0 otherwise. We then evaluated at a type 1 error level of $\alpha = 0.05$, and used the Benjamini-Hochberg procedure to control the false discovery rate [2] for our 318 p-values. All data used in this experiment are provided in the supplemental.

Two-Sample Simulations

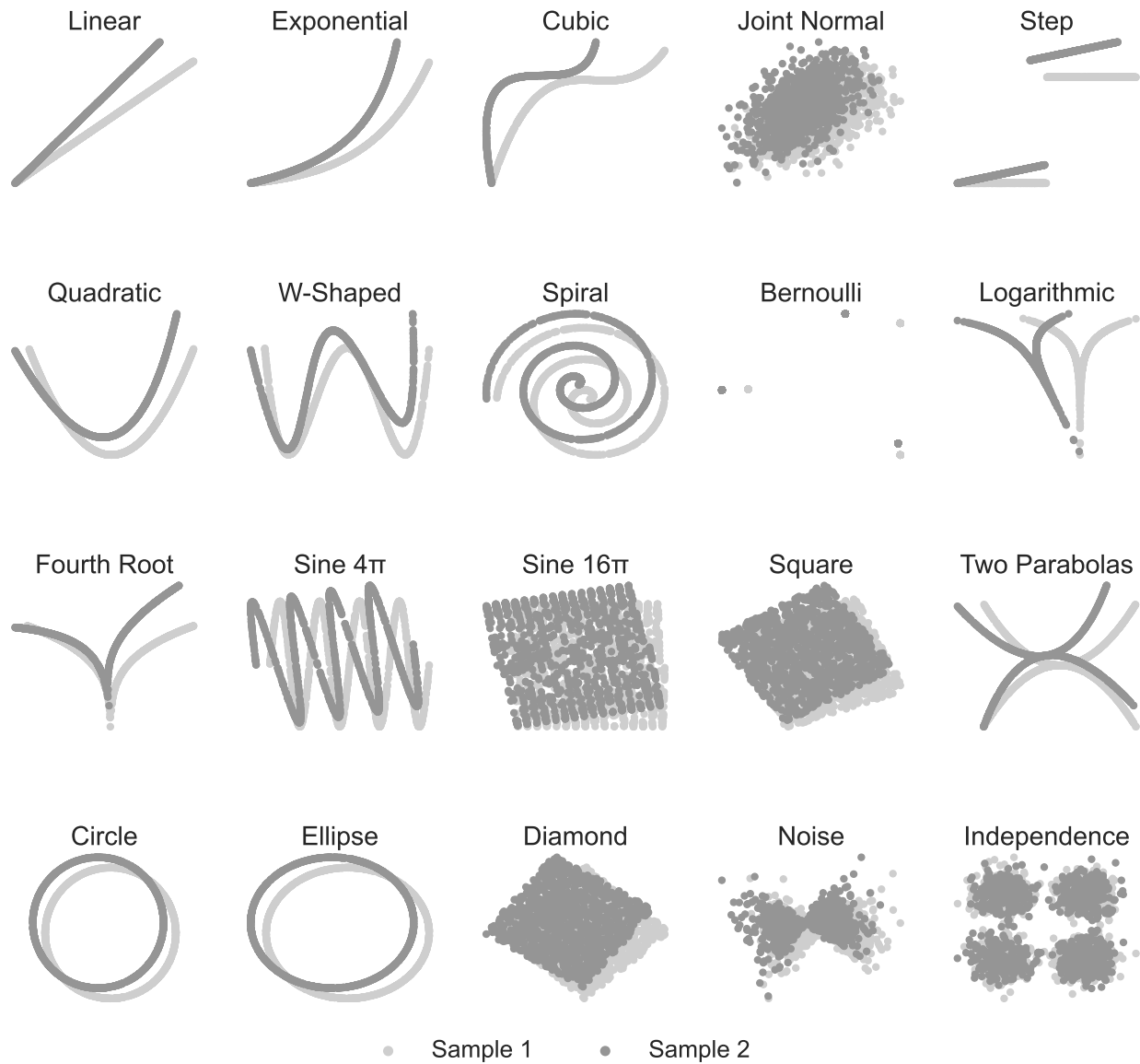


Figure F2: Simulations used for Figure 2. The first dataset (black dots) is 1000 samples from each of the 20 two-dimensional, no-noise simulation settings. The second dataset is the first dataset rotated by 10 degrees counter-clockwise. Simulations were normalized using min-max normalization for visualization purposes.

Appendix E. Hardware and Software Configurations.

- Operating System: Linux (ubuntu 20.04)
- VM Size: Azure Standard D96as v4 (96 vcpus, 384 GiB memory), Azure Standard B20ms (20 vcpus, 80 GiB memory)
- Software: Python 3.8, hyppo v0.4.0